 DOI: 10.1111/j.1539-6924.2011.01602.x

Animal and Human Dose-Response Models for *Brucella* Species

Sondra S. Teske,*[,1] Yin Huang,[2] Sushil B. Tamrakar,[1] Timothy A. Bartrand,[3] Mark H. Weir,[2] and Charles N. Haas[1]

Human Brucellosis is one of the most common zoonotic diseases worldwide. Disease transmission often occurs through the handling of domestic livestock, as well as ingestion of unpasteurized milk and cheese, but can have enhanced infectivity if aerosolized. Because there is no human vaccine available, rising concerns about the threat of Brucellosis to human health and its inclusion in the Center for Disease Control's Category B Bioterrorism/Select Agent List make a better understanding of the dose-response relationship of this microbe necessary. Through an extensive peer-reviewed literature search, candidate dose-response data were appraised so as to surpass certain standards for quality. The statistical programming language, "R," was used to compute the maximum likelihood estimation to fit two models, the exponential and the approximate beta-Poisson (widely used for quantitative risk assessment) to dose-response data. Dose-response models were generated for prevalent species of *Brucella: Br. suis*, *Br. melitensis*, and *Br. abortus*. Dose-response models were created for aerosolized *Br. suis* exposure to guinea pigs from pooled studies. A parallel model for guinea pigs inoculated through both aerosol and subcutaneous routes with *Br. melitensis* showed that the median infectious dose corresponded to a 30 colony-forming units (CFU) dose of *Br. suis*, much less than the N_{50} dose of about 94 CFU for *Br. melitensis* organisms. When *Br. melitensis* was tested subcutaneously on mice, the N_{50} dose was higher, 1,840 CFU. A dose-response model was constructed from pooled data for mice, rhesus macaques, and humans inoculated through three routes (subcutaneously/aerosol/intradermally) with *Br. melitensis.*

KEY WORDS: Brucellosis, dose-response model; microbial risk assessment

1. INTRODUCTION

The genus *Brucella* contains gram-negative, facultative, nonspore forming, intracellular pathogens per Corbel.[1] As a zoonotic disease, the manifestations of *Brucella* are linked to differences between the species and diversity between hosts that can affect any organ and tissue producing protean clinical symptoms. Underdiagnosis of brucellosis is common because it displays nonspecific manifestations that can mimic various diseases depending upon which organ is affected, similar to syphilis. Analysis through blood culture growth is slow ($\geq$7 days) and sensitivity is variable, ranging between 50% and 90% depending on the stage of the disease. Serodiagnosis is complex because antibody readings in cases of relapses of chronic brucellosis are difficult to interpret compared to those of endemically exposed populations.[2–4] Although human brucellosis has low mortality rates, it has significant morbidity and can be an acute or chronic disease. The disease presents with

[1]Department of Civil, Architectural, and Environmental Engineering, Drexel University, Philadelphia, PA, USA.
[2]Water Quality, Environmental, and Molecular Biology Laboratory, Department of Fisheries and Wildlife, Michigan State University, East Lansing, MI, USA.
[3]Tetra Tech Clancy Environmental, Scituate, MA, USA.
*Address correspondence to Sondra Teske, 3141 Chestnut Street, Curtis Hall, PA 19104, USA; ssteske@gmail.com.

 0272-4332/11/0100-0001$22.00/1 © 2011 Society for Risk Analysis

many common symptoms including fever, fatigue, anorexia, sweats, and depression.[5,6] *Brucella* can access the host through ingestion, inhalation, penetration through the skin, or conjunctival contact. However, if it is aerosolized, its infectivity increases.[5] All of these characteristics have qualified this bacteria for inclusion in the Center for Disease Control's (CDC) Bioterrorism Disease/Agents List as a Category B agent and spurred efforts to better understand the mechanisms of this microbe's infectivity, prevent outbreaks, and improve disease treatments.

Genetic analysis has grouped the genus *Brucella* into six different species related to their primary hosts, which include *Brucella melitensis* (derived from sheep and goats), *Br. suis* (hogs), *Br. abortus* (cattle), *Br. ovis* (sheep), *Br. canis* (dogs), and *Br. neotomae* (wood rats).[7] However, newly recognized species include *Br. pinnipedialis* (seals), *Br. ceti* (dolphins, porpoises), *Br. microti* (voles, foxes), and *Br. inopinata* (unknown).[8–10] Of the many species listed, the three with the most pathogenic effect (*Br. melitensis*, *Br. Suis*, and *Br. abortus*) and difficulty in eradication[6,11] will be highlighted in this work.

Brucellosis ranks number one in occurrence among zoonotic diseases in the world with over half a million new cases reported every year, predominantly in Asia, Africa, and near the Mediterranean basin. Brucellosis trends positively with low socioeconomic status, and livestock propagation. Some areas, such as the Middle East and South America, have had a long history of endemic brucellosis that continues into present day. However, 7 of the top 25 countries ranked in order of the highest incidence of brucellosis worldwide used to belong to the Soviet Union.[12] In some of these countries (Albania, Bosnia, Herzogovina, Armenia, Azerbaijan, Turkmenistan, Uzbekistan, Kazakhstan, Tajikistan, Krygyzastan, and Mongolia) political and economic instability have created a resurgence of the disease due to economic dislocations following the disintegration of the Soviet Union. Several researchers have reported that many of the former Soviet-bloc-supported programs for veterinary care, vaccinations, and strict livestock controls have suffered during the switch to underperforming free markets. Lack of funds has also diminished the overall level of healthcare available, affecting patient diagnosis, treatment, disease prevention, and access to medical supplies.[12–15]

Reduction of human brucellosis has best been promoted through elimination of its occurrence in livestock. The disease is commonly transferred through the handling of livestock and its byproducts, as well as ingestion of unpasteurized milk and cheese. This is evidenced by eradication of *Br. abortus* through cattle vaccination in the 1960s whereas previously it had been the most prevalent source of human brucellosis in the United States. In the subsequent decades, *Br. suis* outbreaks among abattoir workers dominated but the overall levels were low.[12,16] However, since the early 1990s, the rising incidences of *Brucellosis* in the United States have been traced back to Hispanic immigrants coming from the mid to northern states of Mexico with pockets of endemic *Br. melitensis* (Sonora, Chihuahua, Coahuila, Nuevo Leon, Sinaloa, Zacatecas, Durango, and Guanajuato).[12] The concomitant rise in foodborne transmission of *Br. melitensis* in the past 20 years is related to the import and consumption of goat cheese, and other dairy products,[12,17] and is reported worldwide as an important transmissive vector as well.[4,12,18] In contrast to some other zoonotic diseases, most researchers have concluded from several epidemiological surveys of various wildlife populations (such as caribou, wild deer, sheep, and boars) that wildlife do not serve as reservoirs of the disease, but are only the occasional victims after contact with domesticated animals.[19] Even though this is fortuitous, the prevalence of brucellosis throughout the world even after the development of livestock vaccines points to the need for both a concerted effort to provide adequate worldwide aid for livestock vaccination programs and the development of a human vaccine. The rising concerns about the threat of Brucellosis to human health and its inclusion in the CDC Category B Bioterrorism/Select Agent List[20] make the understanding of the dose-response relationship of this microbe necessary.[21]

2. DATA AND METHODS

2.1. Dose-Response Data Sources

Druett *et al.*[22] researched the effects of exposing guinea pigs to aerosolized *Br. suis* organisms as reported in Table I with the endpoint of infection. The guinea pigs weighed 350–400 g at the time of exposure and were held for 4 weeks postinoculation before euthanasia. Positive diagnosis for infection was based on organ macroscopic inspection and also by identifiable *Br. suis* colonies growing on agar cultures of the incised surfaces of the spleen, liver, cervical, and bronchial lymph glands of the euthanized tested animal. The mean time to infection was not

Table I. Dose-Response Data of Guinea Pigs Exposed to Aerosol Clouds of Individual Organisms of *Brucella Suis* and Evaluated at 4 Weeks Postinfection as Investigated by Druett *et al.*[22]

	Aerosol Particles' Diameter (μm)	Dose (Organisms-min/L)	Transformed Dose[a] (No. of Organisms-CFU)	Positive Response	Negative Response	Total No. of Subjects
(A)	0.6[b]	82	12	10	30	40
		136	20	13	27	40
		219	32	29	11	40
		364	53	31	9	40
		573	83	35	5	40
(B)	0.6	94	14	4	16	20
		141	20	6	14	20
		227	33	7	13	20
		413	60	22	7	20
		593	86	18	2	20
(C)	0.6	238	34	15	15	30
		363	52	17	13	30
		390	56	23	7	30
		412	60	25	5	30
		519	75	23	7	30
		924	134	30	0	30
(D)	0.6	87	13	6	14	20
		162	23	8	12	20
		280	40	11	9	20
		525	76	13	7	20
		633	91	17	3	20

[a]Original mass flow rate of *Brucella* organisms' data from a nebulizer machine (organisms—min/L) was transformed to dosages inhaled by the test guinea pigs through multiplication of 0.1445 L/min (the ventilation rate). The ventilation rate was estimated based on an average breathing rate of 85 breaths/min multiplied by the tidal volume breathing rate of 1.7 mL/breath, which corresponds to normal ranges for guinea pigs weighing between 350 g and 400 g.[23]
[b]Estimated average diameter (0.5 μm–0.7 μm) of *Br. ceti* and *pinnipedialis* species isolated from marine mammals, genetically and taxonomically related to the six classical nomen species of *Brucella*, including *Br. suis* as reported by Foster *et al.*[40]
Note: All data were successfully pooled.

provided in the study because it was partially dependent upon dosage and particle size. Aerosol exposures (organisms-min/L) of microbial organisms were converted to total dosage by applying the ventilation rates of guinea pigs and mice as reported by Kleinman and Radford.[23] The average breathing rate (85 breaths/min) was calculated from the range of 70–100 given for guinea pigs provided by the same researchers. The breathing rate was combined with the corresponding tidal volume of 1.7 mL/breath (based on the mammal's body weight) to obtain the ventilation rate of 0.1445 L/min with confidence intervals ±15% as mentioned by the author. The ventilation rate (L/min) was multiplied by the aerosol production rate (organisms-min/L) to obtain the total number of organisms in the inoculation. The apparatus used by Druett *et al.*[22] to produce aerosols of individual infective organisms was designed by Henderson.[24] Druett *et al.*[22] estimated that approximately 90% of the droplets as they emerged measured less than 10 μm in diameter. To make clouds with particles $\geq$8 μm, an inert bulking agent (dextrin) was added to the mixture to control the number of organisms while adjusting the size of the particle diameter to what was desired and produced via the Henderson apparatus.

In Elberg and Henderson's study,[25] guinea pigs (weighing between 350 g and 400 g) were exposed to aerosol doses of *Br. suis* and *Br. melitensis*. Euthanasia occurred 30 days postinoculation, with the spleen, liver, lung, and respiratory tract lymph nodes removed for analysis. The organs were ground or minced, and suspended in a tryptose-saline mixture that was applied to tryptose agar for culture. Histopathological examination of sections of the lung and spleen were done as well. Henderson's apparatus was used to generate aerosol particles of specific diameters for the study by Elberg and Henderson[25] and was also utilized by Druett *et al.*[22,26] in their research. However, conversion of the aerosol

generation rates (seen in Druett *et al.*'s paper)[22] were not required for using the data, as estimated dosages were provided by Elberg and Henderson.[25]

Herzberg *et al.*[27] focused on studying the effectiveness of a streptomycin-dependent strain vaccine of *Br. melitensis* against a challenge of the wild type of *Br. melitensis* delivered subcutaneously to both guinea pigs and mice. The control groups tested with the virulent wild-type challenge dose alone were used for the dose-response data. An initial paper by Herzberg and Elberg[28] describing the isolation of the vaccine elucidated in more detail the methods for this test, including that infection was positively identified in each case by spleen culture that was evaluated at 4 weeks after inoculation for guinea pigs (weighing 300–500 g), and at 3 weeks postinjection for male BRVS Webster mice weighing 18–20 g. Spleen preparation and culturing followed the same methods as described by Elberg and Henderson.[25]

Elberg *et al.*[29] extended testing the streptomycin-dependent strain vaccine of *Br. melitensis* reported on by Herzberg *et al.*[27] to rhesus monkeys (*Macacus rhesus*). Although the vaccine was injected subcutaneously (similar to the previous study), the virulent challenge doses of the wild type *Br. melitensis* strain 6015 were administered through aerosol clouds using the same Henderson apparatus used in the other studies above.[24] The number of animals infected was evaluated at several periods postinfection: 14 days, 28 days, 35 days, and 45 days, but only the 4-week and 6-week attack rates were reported alongside the scaled infective doses. A positive determination of infection was from ground tissues (inguinal and axillary lymph nodes, spleen, liver, lung, cervical and bronchial nodes, and heart blood) being suspended in solution, streaked, and cultured on fortified tryptose agar with identifiable *Brucella* organism colony growth after several days. A parallel study tracked the distribution differences of infected tissue related to the same levels of a vaccine along with a challenge dose being administered through an inhalation route, or a subcutaneous route. The control groups for this study presented distinct profiles of allocation between the tissues exhibiting infection.

Foster and Ribi[30] researched the effectiveness of a *Br. abortus* strain 19 vaccine. Male white Swiss mice of the Rocky Mountain Laboratory strain (28 days to 30 days old) were injected with the vaccine, and later dosed intraperitoneally with the challenge strain of *Br. abortus* 2308 and sacrificed 12–15 days later. The control groups used in this study provided the data for the dose response used in this study. Positive identification with *Brucella* infection was indicated by colony-forming units growing after 5 days incubated at 37°C on tryptose agar streaked with the ground mouse spleen suspended in tryptose broth.

Vaccine trials with a *Br. melitensis* Rev I strain, given intradermally and followed for 48 weeks after exposure, were conducted on 10 male human volunteers in a study conducted by Pappagianis *et al.*[31] Clinical symptoms, blood cultures, and serology (agglutinin and complement fixation [CF]) tests were evaluated at least weekly to determine responses to graded dosages of the pathogen. Positive responses for infection were determined by a nonnegative agglutinin Rev I titer, which usually corresponded to a positive CF response as well.

The influence of particle diameter sizes on the modeled dose response was elucidated from the previous study of *Br. suis* by Druett *et al.*,[22] and their earlier research with anthrax spores.[26] The data used for analysis in both studies used the same laboratory subjects (guinea pigs) weighing between 350 g and 400 g and exposed to aerosols generated by the same apparatus under the same conditions.

2.2. Modeling and Analysis Method

Candidate dose-response data as extracted from an extensive literature review had to meet quality standards to determine whether they qualified for inclusion in the analysis. The criteria included a clear description of methods, a mode of exposure, reporting of the number of affected and unaffected subjects, as well as defined criteria for the physiological endpoint (mortality or infection symptoms). A minimum of three dose points with at least one intermediate response (other than 0 or 1) were required. A Cochran-Armitage test of trend was employed to discern whether the data displayed increasing proportions of infection that paralleled higher dosages.[32] When a significant trend was observed, maximum likelihood estimation (MLE) was utilized for fitting the dose-response models.[32]

The statistical programming language "R" (www.r-project.org) was used for the MLE computations to fit two models to dose-response data. These two models, exponential (Equation (1)) and approximate beta-Poisson (Equation (2)) have been widely used for quantitative risk assessment, and depend on a mechanistic predictive dose-response relationship that relies on two assumptions. The

host must ingest one or more organisms capable of causing the disease, but only a fraction of those organisms passing into the body can reach a site of incipient infection due to the host's immune defense system or natural decay of the organism. Thus, the framework of predicting disease development is described as an estimated probability of a number of infectious organisms surviving and successfully initiating infection in the host:[32]

$$P(d) = 1 - e^{-kd}, \tag{1}$$

where $P(d)$ is the probability of response at dose d and k is a rate parameter affecting the dose relating to the probability that a single organism can survive and initiate infection.

$$P(d) = 1 - \left[1 + \left(\frac{d}{N_{50}}\right) \cdot (2^{1/\alpha} - 1)\right]^{-\alpha}, \tag{2}$$

where N_{50} is the median infective dose and α is the slope parameter for the beta-Poisson model.

The exact beta-Poisson model is based on the Kummer confluent hypergeometric function (Equation (3)) as described by Abramowitz,[33] and referenced by Teunis and Havellar[34] as to their applicable limitations in regards to calculating accurate dose-response models:

$$P(d; \alpha, \beta) = 1 - {}_1F_1(\alpha, \alpha + \beta, -d), \tag{3}$$

where ${}_1F_1$ is the Kummer confluent hypergeometric function and d is the dose for the exact beta-Poisson model. Binomial maximum likelihood estimates were used to optimize the fit of the likelihood function by selecting possible parameters for the best fit of the models in order to minimize the deviances of the estimated model to the observed data.[32] Estimates were made using the Broyden-Fletcher-Goldfarb-Shanno algorithm for optimization. Confidence intervals of the parameters for the best-fitting models were determined via bootstrapping with 10,000 iterations. The goodness of fit was evaluated by comparing the minimized deviance of the MLE to the critical chi-squared distribution with $m - n$ degrees of freedom, $df = m - n$ (where df is the degrees of freedom, m is the number of doses, and n is the number of model parameters) at a 95% confidence level (denoted as $\chi^2_{0.95,\, df}$). The approximate beta-Poisson model could be selected as a best-fitting model only if the difference in minimal deviances between the beta-Poisson and the exponential model was greater than the critical chi-square value for a single parameter (1 df). The hypergeometric model (Equation (3)) was run concurrently with the approximate beta-Poisson model (Equation (2)) to check for validity, especially at low doses. For many data sets where $\beta \gg 1$, and $\alpha \gg \beta$, the differences between the approximation errors provided by applying the approximate beta-Poisson as compared to those of the hypergeometric function are negligible. However, errors in the approximate beta-Poisson estimates can become quite large in areas of low dose where there are insufficient data, where there is a chance that the calculated probability can exceed the maximum limit of the single-hit exponential dose-response model of Equation (1) where $k = 1$.[34] Although the hypergeometric is able to evaluate the maximum probability curve, the approximate beta-Poisson parameters are not bound, and their limits of application are ignored. If data were best fit by the approximate beta-Poisson model, graphical plots of the maximal exponential limit probability and the hypergeometric curves were provided alongside for confirmation of the validity of using the approximate beta-Poisson. Maximum limit probability curves were calculated for $k = 1$ in the exponential Equation (1), where every single-hit dose would have the 100% probability of producing infection.

Pooling between data sets underwent the statistical analyses and tests for lack of fit (as described in several publications).[32,35–38] Only successful pooling data sets were listed in tables and graphically represented. Bootstrapped curves are presented alongside the variance distribution of the optimal model equation's parameters. Lack of fit of optimized models to the data was examined for systematic patterns or exceptionally large magnitudes of the data's residual deviances that could contribute to the sum of the residual deviances being above the critical chi-square value. Residual deviances should be small and randomly distributed around a mean of zero. Systematic patterns of the residual deviances can indicate the need of an additional essential parameter (or set of parameters) that is not included in the model. Normal binomial probability histograms for a discrete population data set when compared to a normal binomially distributed population with the same mean and standard deviation should produce a centralized peak in the probability histogram profile that should display limited skew and match the ideal profile within limits.[39] Unidentified additional model parameters or correlation between factors unaccounted for produce a beta-binomial distribution.[32] Overdispersion of replicate responses due to greater variability produces a flattened and broadened curve when compared to a centralized, peaked

Table II. Druett *et al.*[22] Dosage Data for Aerosol Clouds of *Br. suis* with Specific Aerosol Particle Size Diameters and Exposed Guinea Pigs' Responses Assessed at 4 Weeks

Table (Particle Diameter)	Aerosol Particles Diameter (μm)	Dose (Organisms-min/L)	Transformed Dose[a] (No. of Organisms-CFU)	Positive Response	Negative Response	Total No. of Subjects
3	5	38	5	3	37	40
		45	7	8	32	40
		98	14	13	27	40
		116	17	15	25	40
		117	17	21	19	40
		146	21	17	23	40
		188	27	26	14	40
		222	32	27	13	40
		342	49	29	11	40
		747	108	40	0	40
4	7.6	67	10	11	19	30
		116	17	8	22	30
		325	47	14	16	30
		473	68	20	10	30
		1,750	253	22	8	30
		2,290	331	26	4	30
5	12	926	134	1	39	40
		1,020	147	6	34	40
		1,840	266	6	34	40
		1,930	279	6	34	40
		3,390	490	8	32	40
		3,440	497	10	30	40
		4,330	626	18	22	40
		8,790	1,270	14	26	40
		8,850	1,279	15	25	40
		20,700	2,991	29	11	40
		51,500	7,442	31	9	40

[a]Original mass flux data of *Br. suis* were transformed by multiplication of 0.1445 L/min to obtain estimates of the microbial dosage as described by Kleinman and Radford.[23]

Note: Data were run successfully for maximum likelihood estimates (MLE). However, one set of data (Table II) for the dose responses for particle diameters of 2.5 μm did not pass goodness-of-fit test requirements for MLE tests for either the beta-Poisson or exponential models and was excluded from the table. The dose-response data for each of the particle sizes could not be pooled.

profile. Residual deviances are greater in magnitude on average for beta-binomial distributions. However, some anomalously large residual deviances for single data points were identified as outliers and removed from the data set dependent upon passing certain criteria. Deletion of the data point was accepted only if the data point produced statistically significant improvements for the model's fit, but had low leverage on the dose-response parameters as detailed by Haas *et al.*[32]

3. RESULTS AND DISCUSSION

3.1. Best-Fitting Dose-Response Models

Several individual tests of aerosolized individual organisms of *Br. suis* with approximate average diameters of 0.6 μm[40] applied to guinea pigs were reported in the study by Druett *et al.*[22] with their data included in Table I in the subset referenced Tables I(A)–(D). The dose-response data for each of the subset Tables I(A)–(D) were successfully modeled by best-fitting predictive exponential models (see Table III) with minimized deviances ranging from 2.39 to 6.81, well below the minimal critical chi-square distribution of 9.4877 (associated with 4 *df*). The effect of increasing aerosol diameters on dose response were also evaluated by Druett *et al.*,[22] who assessed the percentage of infected guinea pigs for different doses delivered as 2.5-μm, 5.0-μm, 7.6-μm, and 12.0-μm diameter *Br. suis* aerosols (see Table II). However, the data set in Table II for the 2.5-μm diameter-sized particles failed the Cochran-Armitage test of trend and a likelihood test for significance of the fitted dose-response model. In contrast, the MLE

Table III. Dose-Response Modeling Results for Aerosol Clouds of *Br. suis* Including Data from Druett *et al.*[22] and Elberg and Henderson[25] Tested on Guinea Pigs

Brucella Species	Author; Table; Particle Diameter	Host; Route	Best-Fit Model (MLE)	Minimized Deviance	Parameters	*df*	MLE χ^2 a, $m-n$ par	Pooling Δ	Pooling χ^2 0.95, 1
Br. suis	Druett (1956); subset (A); (0.6 μm)	Guinea pigs; individual organisms via aerosol	Exp	5.434445	$K = 0.027796$	4	9.48772904		
Br. suis	Druett (1956); subset (B); (0.6 μm)	Guinea pigs; individual organisms via aerosol	Exp	2.60683	$K = 0.018464$	4	9.48772904		
Br. suis	Druett (1956); subset (C); (0.6 μm)	Guinea pigs; individual organisms via aerosol	Exp	6.80916	$K = 0.022921$	5	11.0704978		
Br. suis	Druett (1956); subset (D); (0.6 μm)	Guinea pigs; individual organisms via aerosol	Exp	2.390586	$K = 0.019061$	4	9.48772904		
Br. suis	Druett-pooled subsets (A)–(D); (0.6 μm)	Guinea pigs; individual organisms via aerosol	Exp	24.6096	$K = 0.022263$	20	31.4104	7.3686	7.8147
Br. suis	Druett 1956); Table 3; (5.0 μm)	Guinea pigs; organisms via aerosol	Exp	10.4656	$K = 0.031966$	9	16.9190		
Br. suis	Druett (1956); Table 4; (7.6 μm)	Guinea pigs; organisms via aerosol	B-P	4.9405	$a = 0.48399 N_{50} = 36.0367$	4	9.4877		
Br. suis	Druett (1956); Table 5; (12.0 μm)	Guinea pigs; organisms via aerosol	B-P	12.6731	$a = 0.7740 N_{50} = 1608.497$	9	16.9190		
Br. suis	Druett-pooled; subsets (A)–(D) & 3; (0.6 μm & 5.0 μm)	Guinea pigs; organisms via aerosol	B-P	36.8668	$a = 3.24005 N_{50} = 26.285$	28	41.3371	6.5819	0.0000
Br. suis	Elberg (1948); subset (B); (0.6 μm)	Guinea pigs; individual organisms via aerosol	B-P	2.7339	$a = 0.78271 N_{50} = 40.779$	2	5.9915		
Br. suis	Elberg (1948); subset (F); (0.6 μm)	Guinea pigs; individual organisms via aerosol	B-P	0.1541	$a = 1.36943 N_{50} = 31.9005$	2	5.9915		
Br. suis	Elberg (1948); subset (G); (0.6 μm)	Guinea pigs; individual organisms via aerosol	Exp	1.4533	$K = 0.020061$	3	7.8147		
Br. suis	Elberg (1948); subset (H); (0.6 μm)	Guinea pigs; individual organisms via aerosol	Exp	0.4923	$K = 0.019792$	3	7.8147		
Br. suis	Elberg (1948); subset (I); (0.6 μm)	Guinea pigs; individual organisms via aerosol	Exp	0.9402	$K = 0.021421$	3	7.8147		
Br. suis	Elberg-pool subsets (B), (F)–(I); (0.6 μm)	Guinea pigs; individual organisms via aerosol	B-P	15.9111	$a = 2.3013 N_{50} = 32.3067$	17	27.5871	10.1374	11.0705
Br. suis	Druett-Elberg; pooling; (0.6 μm)	Guinea pigs; aerosol	B-P	41.8345	$a = 2.7257 N_{50} = 29.8741$	37	52.1923	3.3857	3.8415

B-P = beta-Poisson; Exp = exponential; χ^2 = critical chi-squared distribution at a 95% confidence level for the *df*, where $df = m - n$, and m is the number of doses, n is the number of model parameters; Δ = the difference between the deviance of the pooled common model minus the sum of the subset models' deviances. The Δ must be greater than the critical chi-square distribution (χ^2, $_{0.95,1}$) of the pooled subsets minus the common model to reject the null hypothesis that all the subsets have a common parameter set, and that the pooled common model is statistically significantly better than the individual subsets.

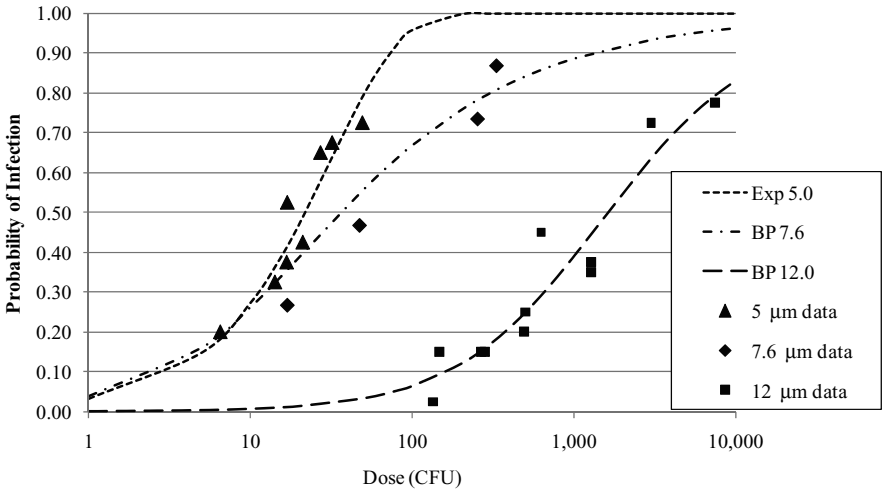

Exp equals predictive exponential dose-response model (Equation (1)); BP equals predictive Beta-Poisson dose-response model (Equation (2)).

Fig. 1. Dose-response data (points) for *Br. suis* aerosols[22] tested on guinea pigs with selected aerosol particle diameter sizes of 5.0 μm, 7.6 μm, and 12.0 μm (Table II) with the best-fitting dose-response models represented by curves. The individual best-fitting dose-response models' fitting parameter values are listed in Table III. The best-fitting exponential dose-response model for 5.0-μm diameter aerosols has a k-fitting parameter of 0.031966 with a minimized deviance of 10.4656, less than the upper χ^2 limit of 16.9190 associated with the 9 *df* in the model. Both the 7.6-μm and 12.0-μm diameter aerosol dose-response data are best represented by beta-Poisson models. The 7.6-μm model's alpha and N_{50} estimates are 0.4839 CFU and 36 CFU, respectively. The 12.0-μm model has an alpha value of 0.7740 and an N_{50} of 1,609 CFU.

results for the other three particle diameter sizes (5.0 μm, 7.6 μm, and 12.0 μm of *Br. suis*) could successfully be fit with the modeled graphs seen in Fig. 1 with the model parameters detailed in Table III. The best-fitting dose-response models for guinea pigs exposed to *Br. suis* aerosols are presented together in Fig. 2 to show a possible relationship between increasing dosage requirements correlating to increases in aerosol diameter size. The two smallest size diameter predictive curves (for the pooled data sets (A)–(D) for individual organisms of approximate average of 0.6 μm and the individual dose-response model for 5.0 μm) are best represented by exponential models with k values ranging from 0.018 to 0.032; specific parameter values are provided in Table III. The larger diameter-sized particles of *Br. Suis* (7.6 μm and 12.0 μm) best-fitting predictive dose-response curves are beta-Poisson modeled.

Druett *et al.*[26] in their anthrax spore research reported a sigmoidal curve with aerosol diameter size (μm) graphed on the horizontal axis, and the N_{50} doses on the vertical axis. Aerosol particles of individual organisms with small diameters exhibited the highest infectivity rates (and corresponding lowest N_{50} dosages). Review of the graphed *Br. suis* aerosol

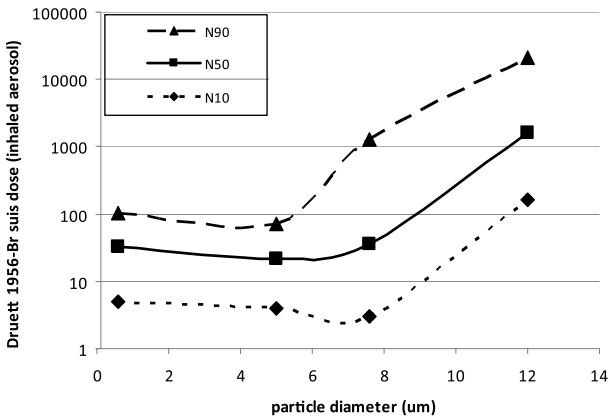

Fig. 2. Effects of different aerosol particle sizes of *Br. suis* on guinea pigs are reflected in the distributions of the N_{10}, N_{50}, and N_{90} doses for the best-fitting dose-response models based on data reported by Druett *et al.*[22] Lines connecting the points are included only for ease of interpretation and do not imply a continuous relationship between points. The N_{10}, median N_{50}, and the N_{90} for the dose-response studies of four different diameter-sized aerosols show that a progressive increase in the required dose is needed to induce the same rate of infection that is initiated for particles with diameters equal or higher than 7.6 μm. Smaller aerosols with diameters of approximately 0.6 μm and 5.0 μm exhibit a lower required dose plateau.

Table IV. Elberg and Henderson[25] Dose-Response Data for Aerosol Clouds of Single Organisms of *Br. suis* Tested on Guinea Pigs with Their Infection Response Measured after 30 Days After Contact

	Dose (CFU)	Positive Response	Negative Response	Total No. of Subjects
(A)[a]	102	11	5	16
	262	19	0	19
	705	16	0	16
(B)	89	13	5	18
	338[b]	14	4	18
	1110	14	1	15
	1950	20	0	20
(C)[a]	145	17	2	19
	345	19	0	19
	870	20	0	20
	2,200	19	0	19
(D)[a]	126	18	1	19
	320	19	1	20
	690	13	0	13
	1,800	20	0	20
(E)[a]	115	16	4	20
	430	18	0	18
	970	18	0	18
	2,460	18	1	19
(F)	26	8	10	18
	58	13	6	19
	97	15	5	20
	320	17	1	18
(G)	21	6	13	19
	49	11	9	20
	108	17	1	18
	270	18	0	18
(H)	22	6	13	19
	53	13	7	20
	108	15	2	17
	228	17	0	17
(I)	24	7	13	20
	40	13	7	20
	117	17	2	19
	270	19	0	19

[a]Data in individual table did not have a minimum of three different dose responses.
[b]Data point (dose 338 in subset B) was excluded from pooled data set.
Note: Each data set (in subsets A–I) was tested individually, and four of them did not have the required minimum of three different doses and responses (subsets A, C–E). Therefore, they were not run for maximum likelihood estimates (MLE) modeling, nor were they included in the successfully pooled set of data.

various 10%, 50%, and 90% infectious dose values (N_{10}, N_{50}, and N_{90}) for the best-fitting modeled dose-response curves in Fig. 2 show a lower plateau of necessary aerosols in colony-forming units (CFU) for particles with diameters less or equal to 5.0 μm, and a steady rise in dosage for particles equal or larger than 7.6-μm diameter to attain the same percent infectivity. The 12.0-μm beta-Poisson N_{50} value (1,609 CFU) is more than 40 times the minimum dosage required to induce a similar infectivity of a 7.6-μm particle diameter of the same agent (Fig. 2).

Experiments run previously by Elberg and Henderson[25] with aerosolized single *Br. suis* organisms (average of 0.6-μm particle diameter) were tested on guinea pigs, similar to the experiments run by Druett *et al.*[22] A series of tests produced several groups of similar dose-response data subsets of usually four dose levels that ranged in each data set from 21 to 2,460 CFU (data sets A–I listed in Table IV). Some of the single data subsets did not pass the criteria standards for data qualification and so were omitted from dose-response modeling and pooling as well (data sets A, C–E in Table IV). Individual dose-response models were created for data sets B and F–I (Table V) were represented by both best-fitting beta-Poisson models (for data sets B and F) and exponential dose-response models (for data sets G–I). The N_{50} estimates for the two beta-Poisson models (data sets B and F) were different (26 and 40, respectively), but the k-parameter values for the exponentially modeled data sets G–I displayed less variability (0.019–0.021), which would equate to an N_{50} between 33 and 36 CFU through the relationship[32] where:

$$N_{50} = \ln(0.5)/-k.$$

The same group of investigators[25] ran trials of aerosol infection of guinea pigs with individual organism clouds of *Br. melitensis*, another species of *Brucella*, with the experimental results registered in Table V. The best-fitting dose-response model was an exponential prediction with the rate parameter $k = 0.0069$ (Table VI).

The effects of an alternative route of administration (subcutaneous injection) was investigated by Herzberg *et al.*,[27] who tested a range of *Br. melitensis* doses on exposed guinea pigs (data in Table V). The optimum dose-response model produced was an exponential model, as well, with $k = 0.0084$ (Table VI).

Herzberg *et al.*[27] evaluated dose responses of mice to subcutaneous inoculation of *Br. melitensis* in coordination with their work on guinea pigs. The administered concentrations of the microbe and the rate of infection in the rodents were evaluated at 3 weeks postexposure (Table V). The best-fitting model for this data group was the beta-Poisson

Table V. Dose-Response Data for *Br. melitensis* and *Br. abortus* MLE Modeling from Various Studies

Study	*Brucella* Species	Exposure Route	Test Subject	Postexposure Evaluation	Table	Dose (CFU)	Positive Response	Negative Response	Total No. of Subjects
Elberg (1948)	*Br. Melitensis*	Aerosol	Guinea pigs	30 days	3.2	18	1	16	17
						45	10	10	20
						109	11	9	20
						270	13	5	18
Herzberg (1953)	*Br. Melitensis*	Subcutaneous	Guinea pigs	4 weeks	4	59[a]	8	1	9
						96	8	2	10
						190	6	4	10
						590	10	0	10
						960	9	0	9
						1,900	10	0	10
						5,900	10	0	10
						19,000	6	0	6
Herzberg (1953)	*Br. Melitensis*	Subcutaneous	Mice	3 weeks	1	3,500	3	3	6
						4,100	5	5	10
						7,500	14	6	20
						350,000	5	2	7
						410,000	7	3	10
						750,000	18	2	20
						35,000,000	7	0	7
						41,000,000	9	1	10
Elberg (1955)	*Br. Melitensis*	Aerosol	Rhesus macaques (*Macaca rhesus*)	4 weeks	1	600	0	10	10
						954	0	10	10
						1,520	2	4	6
						14,500	5	0	5
						122,000	4	0	4
				6 weeks	1	600	3	7	10
						954	4	6	10
						1,520	3	1	4
						14,500	5	0	5
						122,000	4	0	4
Pappagianis(1966)	*Br. Melitensis*	Intradermal	Humans	9 weeks	1	10,000	3	0	3
						20,000	3	0	3
						28,000	1	0	1
Foster (1962)	*Br. Abortus* 2308	Intraperitoneal	Mice	2 weeks	2	10,7000	5	0	5
						10,700	5	0	5
						1,070	5	0	5
						107	4	1	5
						10.7	2	3	5
						1	1	4	5

[a]Data point (dose 59 in Herzberg's Table 4) that was excluded from pooled Elberg-Herzberg data set.

Table VI. Modeling Results for Mechanistic Dose-Response Relationships and Successful Best-of-Fit Maximum Likelihood Estimates and Pooled and Bootstrapped *Br. melitensis* and *Br. abortus* Data

Brucella Species	Author; Table	Host; Route	Best-Fit Model (MLE)	Minimized Deviance	Parameters	*df*	MLE χ^2 a, $m-n$ par	Pooling Δ	Pooling χ^2 0.95,1
Br. melitensis	Elberg (1948); Table 3.2	Guinea pigs; individual organisms via aerosol	Exp	7.3441	$k = 0.00693$	3	7.8147		
Br. melitensis	Herzberg (1953); Table 4[a]	Guinea pigs; subcutaneous injection	Exp	4.8535	$k = 0.008409$	6	12.5916		
Br. melitensis	Elberg (1948)—Herzberg pooling	Guinea pigs; aerosol/ subcutaneous	Exp	12.5662	$k = 0.007349$	10	18.3070	0.3686	3.8415
Br. melitensis	Herzberg (1953); Table 1	Mice (3 weeks); subcutaneous injection	B-P	3.9721	$a = 0.19433 N_{50} = 1840.22$	6	12.5916		
Br. melitensis	Elberg (1955)	Rhesus macaques; aerosol; evaluate at 4 weeks	Exp	6.4139	$k = 0.00014813$	4	9.4877		
Br. melitensis	Elberg (1955)	Rhesus macaques; aerosol; evaluate at 6 weeks	Exp	0.4420	$k = 0.000628$	4	9.4877		
Br. melitensis	Elberg (1955)—Herzberg pooling	Mice rhesus macaques; subcutaneous aerosol	B-P	7.4382	$a = 0.21243 N_{50} = 1923.89$	10	18.30704	3.024125	3.841459
Br. melitensis	Pappagianis (1966)	Human (9 weeks)	Exp	0.6754	$k = .00007966$	2	5.991465		
Br. melitensis	Elberg (1955)—Herzberg-Pappagianis pooling	Mice rhesus macaques (6 weeks) humans	B-P	8.1229	$a = 0.214149 N_{50} = 1885.47$	13	22.36203	3.0334	5.9915
Br. Abortus	Foster (1962)	Mice; intraperitoneally	Exp	4.1878	$k = 0.02475$	5	11.0705		

[a]Modeled result is based on a data set that excluded a certain outlier data point. This adjusted data set was used to pool data for a bootstrapped estimate. B-P = beta-Poisson; Exp = exponential; χ^2 = critical chi-squared distribution at a 95% confidence level for *df*, where $df = m - n$, m is the number of doses, n is the number of model parameters; Δ = difference between the deviance of the pooled common model minus the sum of the subset models' deviances. The Δ must be greater than the critical chi-square distribution ($\chi^2, {}_{0.95,1}$) of the pooled subsets minus the common model to reject the null hypothesis that all the subsets have a common parameter set, and that the pooled common model is statistically significantly better than the individual subsets.

equation (Table VI). The N_{50} for mice with this particular pathogen is much greater than that of guinea pigs receiving inoculation subcutaneously in parallel; 1,840 organisms as compared to approximately 82 CFU. He noted that guinea pigs as compared to mice are extremely susceptible to infection by *Brucella* species via a variety of exposure routes with fewer initiating infectious organisms required to achieve the same response. Mice are much more easily immunized against *Brucella* than guinea pigs as well.

Elberg *et al.*[29] attempted to achieve a stable vaccine against *Br. melitensis* by extending their research subjects to rhesus macaques whose responses to aerosol infection were assessed at 4 weeks and 6 weeks (Table V). Both information sets were best characterized by exponential predictive curves (Table VI).

Physiological and serological test results from vaccine trials of *Br. melitensis* Rev I[31] on human volunteers were recorded for 44 weeks. The data for week 9 postexposure (in Table V) were selected for modeling because they were registered as the first time maximum response attained for those doses with sufficient multiple tested subjects. An exponential model with the rate parameter $k = 0.00007966$ provided the best-fitting model for these subjects (Table VI).

Mice were the test subjects for analyzing the effects of intraperitoneally delivered *Br. abortus*[30] and assessed 2 weeks postinoculation (data listed in Table V). Likelihood statistics indicated that the data could best be fit to an exponential model (Table VI) with the rate parameter $k = 0.02475$ with an approximate N_{50} of 28 CFU.

3.2. Pooling Between Data Sets

All the data from Table I for guinea pigs exposed to individual *Br. suis* organisms (with aerosol particle diameters estimated at 0.6 μm) reported by Druett *et al.*[22] (as Tables I(A)–(D)) were able to be pooled with an exponential best-fitting dose-response model as seen in Fig. 3 with the rate parameter $k = 0.022263$, and its associated N_{50} approximation equal to 31 CFU (listed in Table III).

Progressive pooling of the different data sets of the four separate particle diameter sizes (individual organisms of 0.6 μm through 12 μm) for *Br. suis* was not possible. Some research shows that different sized particles are processed through different physiological regimes and processes of the body's

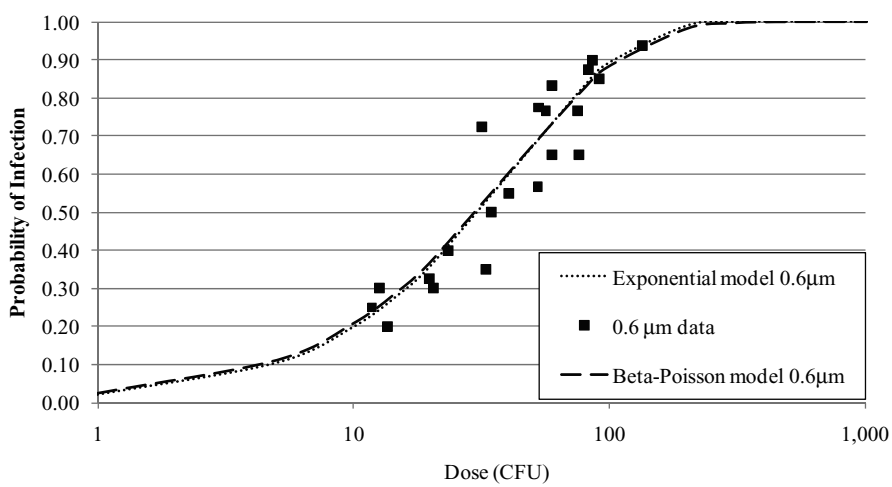

Fig. 3. Pooled dose-response data (Table I) and predictive model results (with parameters listed in Table III) from studies conducted by Druett *et al.*[22] of the effect of individual 0.6-μm diameter organisms of *Brucella suis* given in aerosol clouds to guinea pigs. Although both the exponential model (Equation (1)) and the beta-Poisson model (Equation (2)) display coincident predictive curves, the best-fitting mechanistic model was an exponential model because it had both a minimal number of parameters (one variable, k) and a minimized deviance of 22.5377 (Table III) that was lower than the critical chi-square distribution (χ^2) for 20 df, which was 31.4104. The sum of the four individual best-fitting dose-response models' deviances (from Druett *et al.*'s Tables I(A)–(D)) equaled 15.0193 and their summed number of parameters totaled 4. Subtracting the summed models' total deviance from the combination model's deviance of 22.5377 left a remainder of 7.5184 (the pooling Δ). This was less than the critical chi-square distribution of 7.8147 associated with the difference of 3 parameters between the summed models' total parameters (4) minus the pooled model's single parameter. In summary, the pooled model's χ^2 shows significant improvement over the collective χ^2 of the individual models.

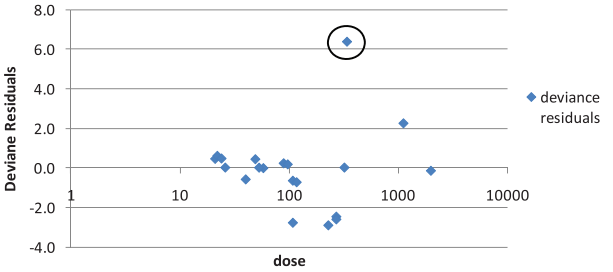

Fig. 4. Residual deviances plotted for pooled aerosolized *Br. suis* dose-response data for guinea pigs from studies conducted by Elberg and Henderson.[25] No systematic bowing or trend of the deviances is notable. However, the residual deviance for dose 338 (circled) was higher than any of the other data points and prevented the collective data from conforming to the goodness-of-fit test. With elimination of this anomalous point, the combined sets of dose-response data successfully passed the significance of pooling test and statistically conformed to a beta-Poisson model (Tables III and IV).

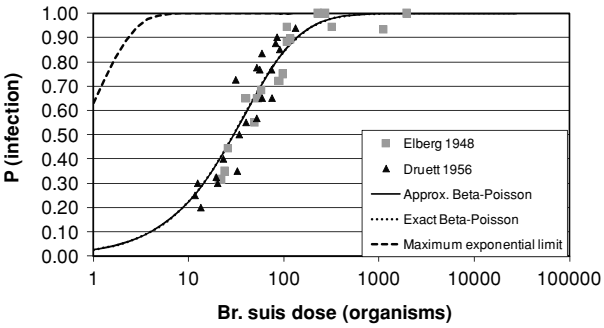

Fig. 5. Pooled dose-response data for individual organisms of *Br. suis* given in aerosol form to guinea pigs from studies conducted by Elberg and Henderson[25] and Druett *et al.*[22] (Tables I, III, and IV).

immune system producing differential levels of infectivity/lethality.[26,41,42] Only Druett *et al.*[22] data sets from the two smallest-diameter aerosols (the individual organism 0.6 μm-pooled Tables I(A)–(D), and the 5.0-μm data from Table III) were successfully pooled with a best-fitting beta-Poisson model with an alpha value = 3.24 and an N_{50} of 26 CFU (Table III). It seems possible that the clumping agent (dextrin) used to decrease the numbers of organisms per droplet and create larger particle sizes may interfere with the physiological infectious processes. Whatever the cause, however, pooling between the two remaining larger *Br. suis* diameter aerosol particle data sets (for 7.6 μm and 12.0 μm) was not successful, so their infectious rates are distinct.

Combining the similar data set of guinea pigs exposed to aerosolized *Br. suis* data reported by Elberg and Henderson[25] for individual organisms in table subsets (B), and (F)–(I) (listed in Table IV) was attempted, but successful pooling of the collective group was not possible without the elimination of a single outlier data point, dose 338 (in data subset B, Table IV, marked by indicator [a]) although the individual data sets' iterative process successfully converged. The residual deviance for this dose measured much higher than the other data points, as evidenced by the plot in Fig. 4. As the residual deviances of the other data did not exhibit significant trends or patterns such as bowing, or linear related increases with dose that may point to an undiagnosed factor in the relationship, the anomalous data point was removed from the collective pooled data for analysis. The successfully pooled data that now conformed to the statistical requirements outlined previously and the best-fitting dose-response model was a beta-Poisson curve in contrast to the best-fitting exponential model based on Druett *et al.*'s[22] data (Fig. 3; Tables I and III).

A second level of pooling was achieved when the aerosol *Br. suis* data for guinea pig exposure from Druett *et al.*[22] and Elberg and Henderson[25] (Tables I and IV) were able to be successfully pooled with model parameters $\alpha = 2.7257$ and $N_{50} = 29.87$ CFU (Table III). Equal distribution of data points about the resulting pooled MLE approximate beta-Poisson model predictive curve can be observed (Fig. 5). In addition, the exact beta-Poisson (hypergeometric) model is confluent with the approximate beta-Poisson model and does not overlap the maximum exponential limit line at low doses.

A valid exponential dose-response model for the experimental infection of guinea pigs through two routes of *Br. melitensis* was created from pooling two data sets with different administration routes: aerosols, researched by Elberg and Henderson,[25] and subcutaneous injection, reported by Herzberg *et al.*[27] (Table V). However, removal of an outlier point (dose 59 in Herzberg *et al.*'s[27] data set 4, Table V) was required subsequent to scrutiny of the deviance residuals of both the exponential and beta-Poisson dose-response models (graphed, respectively, in Figs. 6 and 7) to promote successful pooling of the two data series.[25,27] The best-fitting exponential model common to the combined data sets has a k-parameter value of 0.007349, which corresponds to an N_{50} estimate of 94.3 CFU (Fig. 8; Table VI). The estimated 50% infectious dose

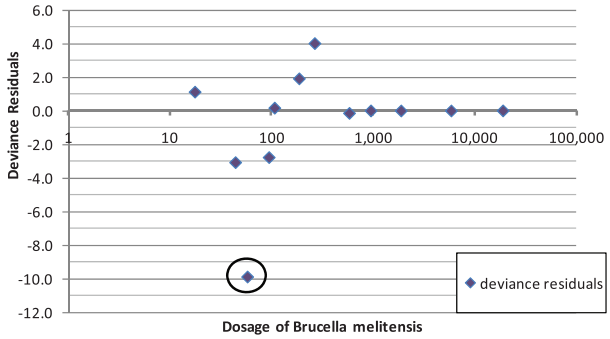

Fig. 6. Residual deviances plotted for exponential model (Table VI) of pooled dose-response data for guinea pigs exposed to aerosols[25] or subcutaneous injection[27] of *Br. melitensis*. Circled residual deviance is for dosage 59 (Table V) and its related response reported in the data set for subcutaneous injection by Herzberg *et al.*[27] and deleted as an outlier.

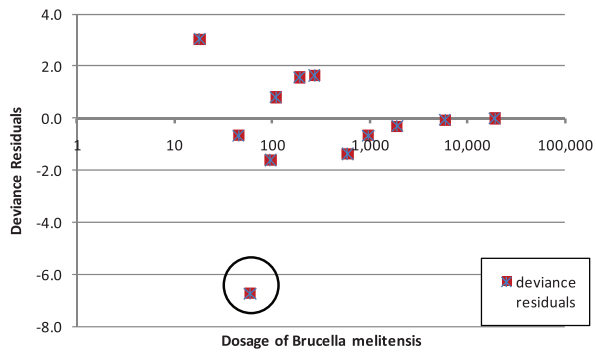

Fig. 7. Residual deviances plotted for beta-Poisson model of pooled Herzberg *et al.*[27] and Elberg and Henderson[25] dose-response data for guinea pigs' subcutaneous injection and aerosol inhalation (respectively) of *Br. melitensis* with subsequent evaluation at 4 weeks. Circled residual deviance is for a data point from Herzberg's data (Table V). In both models (Table VI), this data point is an outlier, and was deleted for final pooled data set.

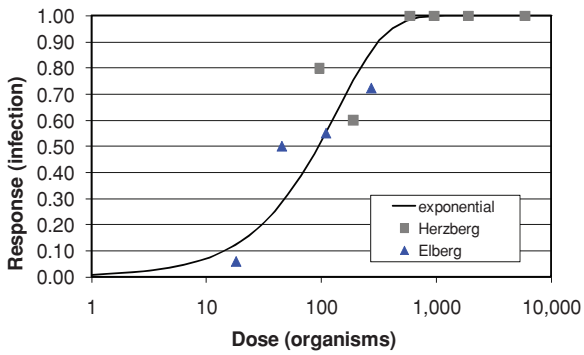

Fig. 8. Pooled guinea pig dose-response data for *Brucella melitensis* with exposure by aerosol, researched by Elberg and Henderson,[25] and via subcutaneous injection, tested by Herzberg *et al.*,[27] with best-fitting exponential model predictive plot (Table VI).

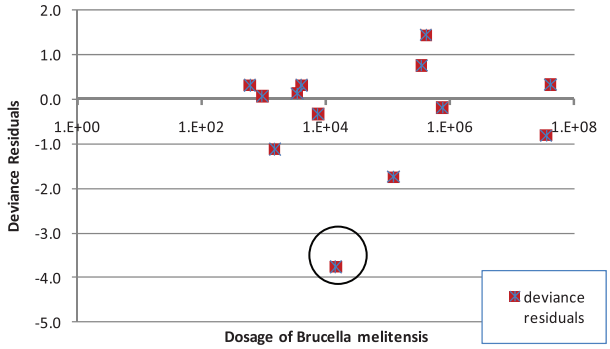

Fig. 9. Residual deviances for pooled dose responses for beta-Poisson model for rhesus macaques[29] and mice[27] (Table VI) exposed to *Br. melitensis* with outlier dosage of 14,500 circled due to its anomalously high residual deviance (Table V).

(ID_{50}) for *Br. melitensis* is approximately 60 organisms higher than that required for *Br. suis* for the same test subjects (guinea pigs). Model fitting and parameter results for the pooled and bootstrapped models are listed in Table VI.

Pooling between the 4-week and 6-week experimental infection outcomes for the *Br. melitensis* exposed rhesus macaques conducted by Elberg *et al.*[29] was not possible. In addition, pooling between the rhesus macaque and guinea pig test results for *Br. melitensis* vapor exposure was not statistically viable. However, successful pooling between mouse dose-response data[27] and the 6-week data for rhesus monkeys[29] could be realized after removal of an outlier data point (Fig. 9) with dose 14,500 CFU from Elberg *et al.*'s[29] data (Table V). The best-fitting beta-Poisson model (shown in Fig. 10) had an N_{50} dose approximation of 1,924 CFU.

Results from the human vaccine trials of *Br. melitensis* Rev I[31] were pooled with the pooled mice-rhesus macaque *Br. melitensis* data successfully as well, with very small differences observed in the statistical parameters. The 50% infectious dose estimate was 1,885 CFU (Table VI). The exact and approximated beta-Poisson models coincided and did not intersect the maximum exponential limit curve at any dose, which means that the approximate beta-Poisson model is suitable for use with this data set.[34] This model establishes that this model of a mechanistic dose response can link correlations between not only different administration routes (subcutaneous injection, intradermal, and aerosol), but more importantly, establish parallel infectious disease processes between two distantly related animal species and humans.

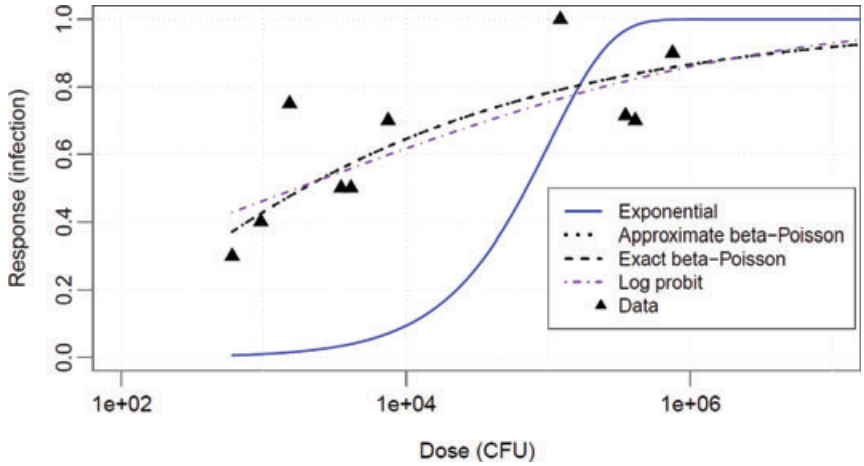

Fig. 10. Pooled dose response for rhesus macaques[29] and mice[27] exposed to *Br. melitensis* with omission of one data point (Tables V and VI). The exact beta-Poisson and approximate beta-Poisson model curves are very similar.

3.3. Bootstrapped Results

All individual data sets were bootstrapped (and are available upon request from the author) but only the most representative or widely applicable bootstrapped data sets will be discussed and presented.

The bootstrapped pooled data sets from Druett *et al.*[22] and Elberg and Henderson[25] for guinea pigs tested by single aerosolized organisms of *Br. suis* are plotted with optimized parameters for the beta-Poisson model (Fig. 11) and exhibit narrow and closely aligned 95% and 99% confidence intervals.

The pooled data sets of the similarly designed experimental infection of guinea pigs exposed to aerosols of another species, *Br. melitensis*,[25] were combined with data of the same subjects' responses tested through subcutaneous injection[27] and optimized through the bootstrap procedure to produce an exponential model (Fig. 12). The 95% and 99% projected confidence intervals derived from the bootstrapped estimates display a narrow range, and the frequency distribution of the exponential parameter k shows a normal distribution with limited skew (Fig. 13).

The pooled *Br. melitensis* monkey (aerosol)-mouse (subcutaneous) data set is best represented by an approximate beta-Poisson model (Fig. 10) that is confluent with the modeled exact hypergeometric model and is represented by Fig. 14, with final parameter and fitting results detailed in Table VI. Expansion of this monkey-mouse model by inclusion of the data for intradermal dispensation of *Br. melitensis* to humans created almost a replicate predictive model (Fig. 15).

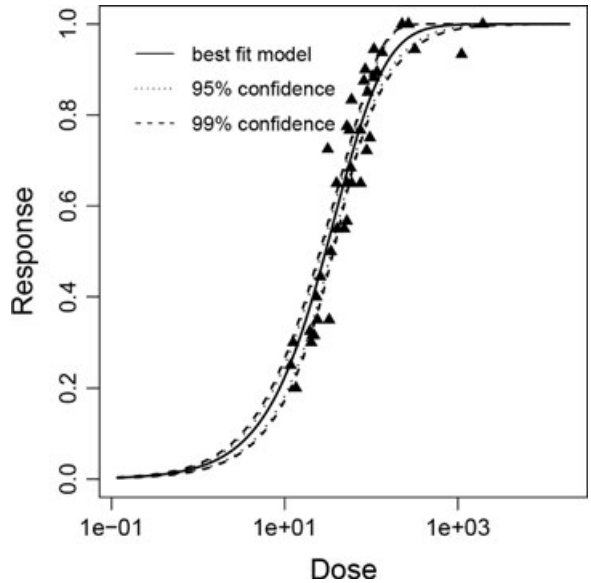

Fig. 11. Bootstrapped and optimized best-fitting beta-Poisson model ($\alpha = 2.7257$; $N_{50} = 30$ CFU) predicting the pooled dose-response data for guinea pigs exposed to aerosols of single-spore organisms (with approximate particle diameters of 0.6 μm) from research conducted by Druett *et al.*[22] and Elberg and Henderson.[25]

The only data available for representing the infectious disease process for another species of *Brucella*, *Br. abortus*, were investigated by Foster and Ribi.[30] The effects of the infection, which was intraperitoneally delivered to mice, was assessed 2 weeks postinoculation. Likelihood statistics indicated that the data could best be fit to an optimized exponential model (Table VI). The resulting

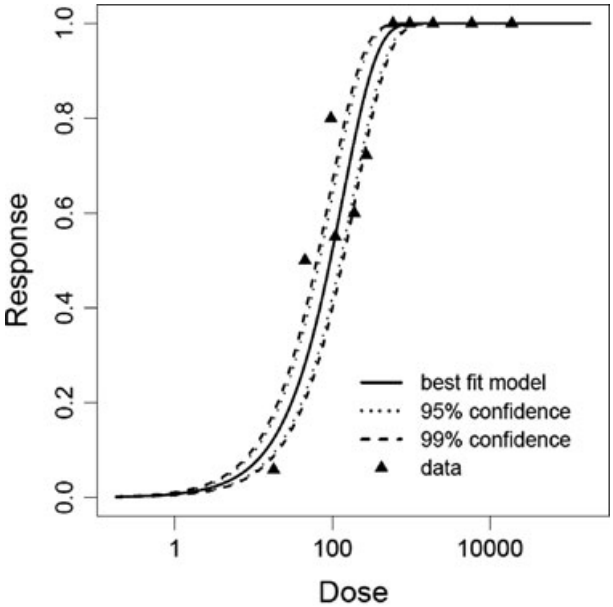

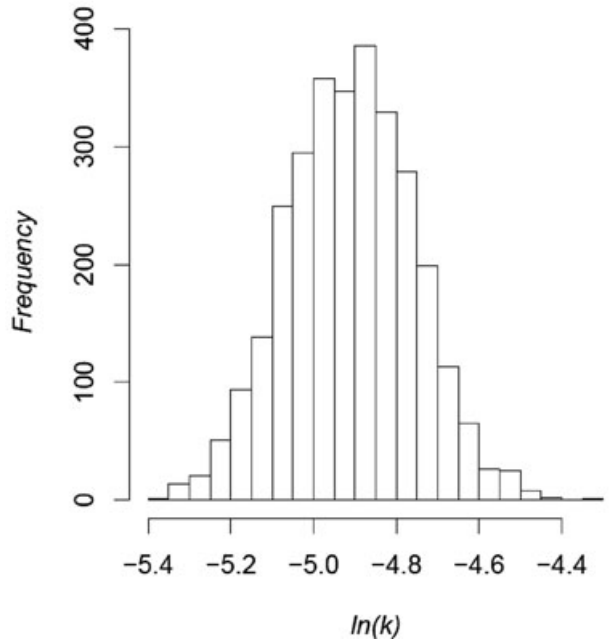

Figs. 12 and 13. Bootstrap results graph for guinea pig exposed to *Br. melitensis* by aerosol[25] and subcutaneous injection[27] along with frequency diagram of exponential model parameter k (Table VI). Estimated 50% infectious dose is 94 CFU.

bootstrapped results and confidence levels are plotted in Fig. 16, along with the frequency distribution of the exponential parameter k shown in Fig. 17. The extrapolated ID_{50} was 28 CFU, significantly lower than the ID_{50} of 1,840 CFU for mice subcutaneously

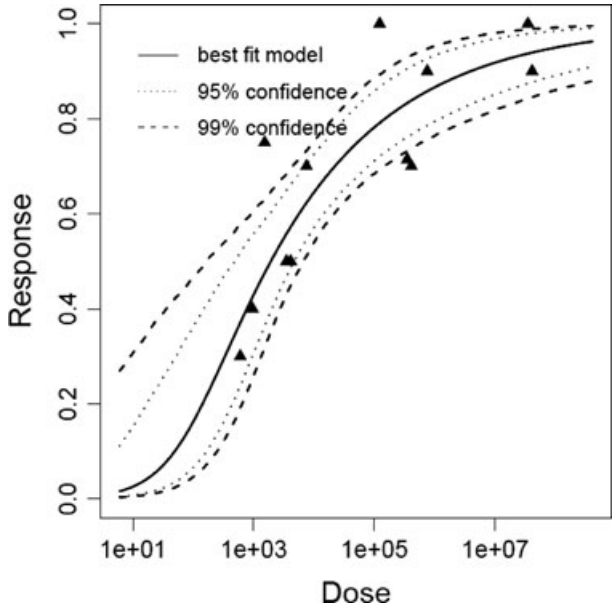

Fig. 14. Bootstrapped beta-Poisson model ($\alpha = 0.21243$, $N_{50} = 1{,}924$ CFU) for pooled dose response for rhesus macaques[29] and mice[27] exposed to *Br. melitensis* with omission of one data point (Table VI).

injected with *Br. melitensis* and assessed 1 week later (at 3 weeks).

3.3.1. *Analysis of Outbreak Data*

An outbreak of *Br. abortus* from an accidental breakage of a polystyrene centrifuge tube at a university laboratory outside of a biological safety cabinet was described in a study done by Fiori *et al.*[43] Although evacuation was instituted immediately, and germicidal remediation measures were completed as per standard safety recommendations, 12 of 39 employees seroconverted within 24 weeks of the exposure. The *Br. abortus* biotype 1 strain was diagnosed through the Rose Bengal microagglutination test. The overall attack rate of 31% indicated that the initial exposure dosage was approximately 10 CFU (Fig. 16; Table VI). Unfortunately, a time postinoculation (TPI) model was not available for this *Brucella* species, so time-related comparisons could not be made for this study.

3.4. Physiological Aspects of *Brucella*

The ability to pool data sets for the same *Brucella* species (*Br. melitensis*) across differently administered routes (through aerosol inhalation and

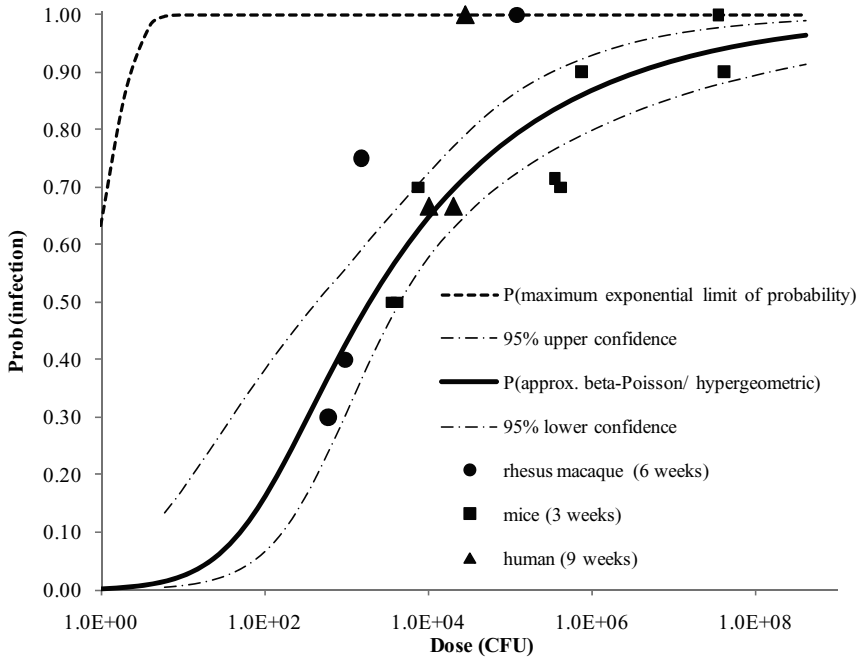

Fig. 15. Bootstrapped dose-response model with confidence intervals for pooled data from three data sets: rhesus macaques (evaluated at 6 weeks),[29] mice (3 weeks),[27] and humans (9 weeks)[31] all exposed to *Br. melitensis* (Table VI). Exact beta-Poisson (hypergeometric) and approximated beta-Poisson best-fitting model curves coincide with an alpha value of 0.214149, and an $N_{50} = 1{,}885$ CFU

subcutaneous injection) to the same test animals (guinea pigs) at about the same evaluation time post-exposure (4 weeks and 30 days) does not seem remarkable because the determination of positive infection relied on the same method of detection. Additionally, pooling for *B. melitensis* data for rhesus monkeys via aerosol (evaluated at 6 weeks) and mice via subcutaneous (measured at 3 weeks) does not seem unreasonable for a number of reasons as well. In all cases, the test subject's spleen was extracted, ground, diluted, and streaked on a tryptose agar plate and similarly cultured/incubated under similar conditions. Growth of *Br. melitensis* colonies after several days' incubation confirmed infection. The antibody response seen in the positive agglutinin titers for the human trials would precede culture of viable brucellae in the spleen, so it is not unexpected that the human data could correspond to dose-infection responses for the mice and rhesus macaques. However, in a comparative trial between inhalation (a control group of 10 rhesus macaques) and subcutaneous injection (a control group of 8) as a determining factor for differences in tissue localization of *brucellae* 6 to 8 weeks after virulent *Br. melitensis* exposure, detection through spleen and inguinal and axillary lymph nodes provided the most reliable positive results no matter which administration route was used.[29] The percentage of animals that were found to have brucellae in the spleen following aerosol exposure was 100%, whereas only 75% of them were positive that were inoculated subcutaneously (Fig. 18). For the inguinal and axillary nodes, 80% of the inhalation route subjects presented microbial traces, less than the 87.5% of the injection group. Distribution of brucellae in the liver, lung, cervical and bronchial nodes, and heart blood was always higher in those animals that received it via respiration as compared to those who received it intradermally. It is interesting to note that bacteremia as an indicator was the least reliable—only half of the subjects exposed through aerosol-exhibited brucellae in heart blood, and only 12% of those administered the toxin subcutaneously showed positive cultures.

The small numbers of culturable brucellae found in blood compared to CFU counts per gram of cultured spleen, liver, and lung tissues at 9 weeks postexposure to aerosol at the same inoculation doses was confirmed by another study on *Br. melitensis* infection of another species of rhesus macaques (*Macaca mulatta*) conducted by Mense *et al.*[44] Bacteremia is only detectable at 21 days after inoculation of 10^5 CFUs, with the majority of test subjects initially testing positive at minimum doses of 10^3 post-exposure 28 days. Inoculation with 10^2 CFUs of the agent did not produce bacteremia even after 63 days; in contrast, the same inoculation dose produced

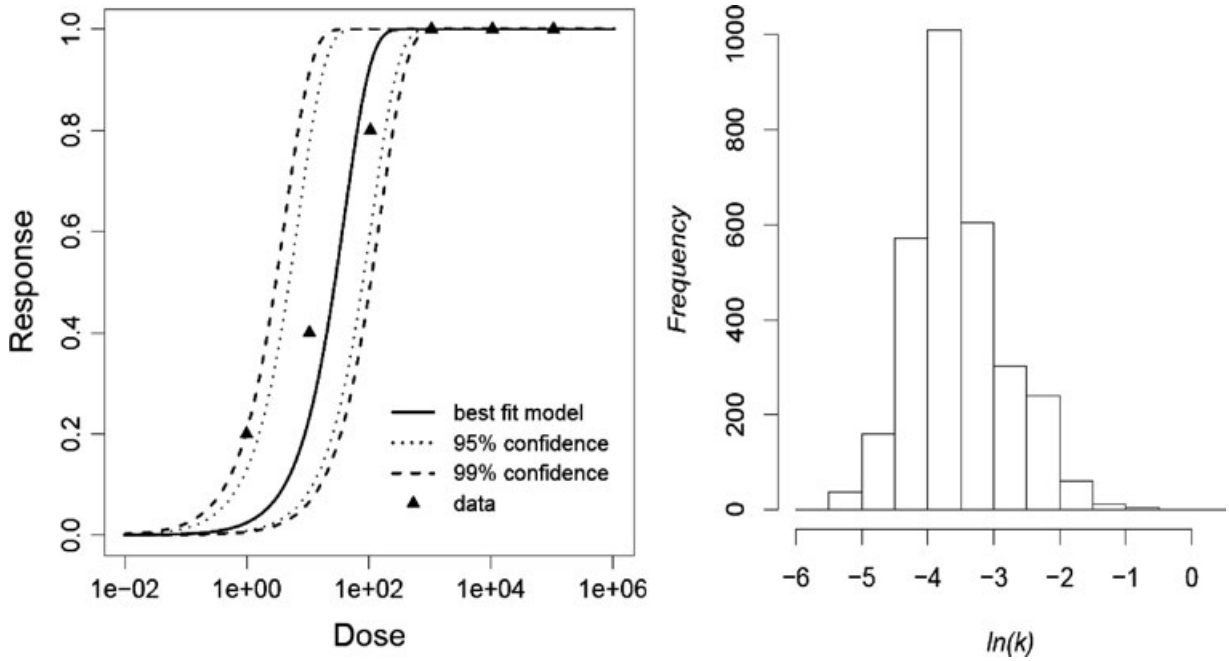

Figs. 16 and 17. Bootstrapped exponential dose-response infection model (Table VI) for mice administered *Br. abortus* strain 2308 intraperitoneally (Fig. 16), and the associated exponential frequency distribution (Fig. 17; Table V).[30] The fitting parameter k was equal to 0.02475, which corresponds to 50% predictive infectious dose of 28 CFU.

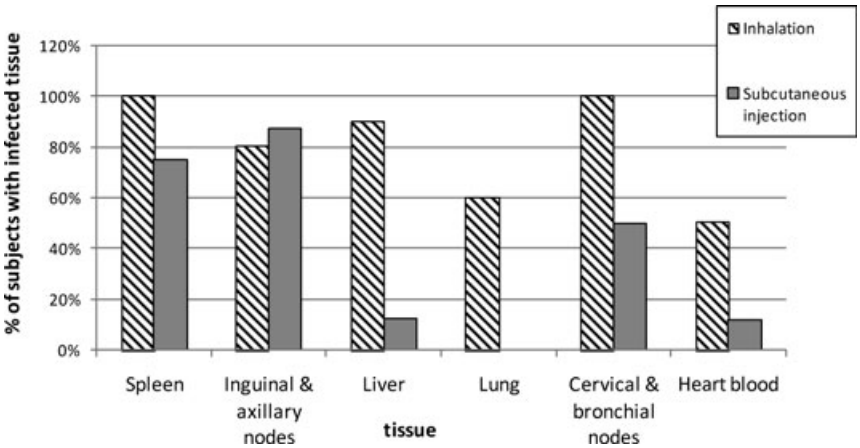

Fig. 18. Distribution of *Br. melitensis* in tissues of rhesus macaques 6–8 weeks after exposure through inhalation or subcutaneous administration routes.[29] Columns represent the percentage of rhesus macaques in the test groups that presented *Brucellae* in those tissues.

histologic lesions causing splenic hyperplasia and hepatitis (liver inflammation). Bacteremia is not a reliable indicator of brucellosis infection in humans as it commonly produces false negative results as compared to liver/lymph node aspirates.[45]

Quantification of *Br. melitensis* tissue distribution between a virulent strain (16 M) as compared to a vaccine candidate (strain WR201) was conducted on male BALB/c mice with oral inoculation by Izadjoo *et al.*[46] At day 3, and weeks 1, 2, 4, 8, and 12, mice were euthanized, and the organs macerated, streaked, and cultured/incubated for detection of brucellae CFU growth. The examined organs included the lung, liver, spleen, testis, epididymis, inguinal, and cervical lymph nodes. For mice, the peak growth of brucellae was seen in the spleen, followed by both the liver and lung CFU counts. Although brucellae counts were not provided for the other analyzed organs, attack rates were provided and the inguinal lymph nodes and testis exhibited higher percentage of subjects infected than for the epididymis and the cervical lymph nodes. The virulent strain

16M displayed higher intensity and longer duration of infection than the WR201 strain (a human vaccine target) of *Br. melitensis.* Because the male genitorurinary system is targeted by virulent *Brucella* strains in humans and livestock, Izadjoo proposed that male mice are a relevant animal model for evaluating pathogenesis of the disease.

Work done on *Br. melitensis* propagation and distribution in tissues conducted by Olsen *et al.*[47] shows that at nearly every dose level, the total CFU per gram of tissue culture in 10-week-old female BALB/c mice exhibited higher concentrations of brucellae in the spleen, followed by the lung and the liver when evaluated at 2 weeks postexposure, similar to conclusions noted by other studies. A parallel test run on exposing the same mice to the same dose ranges of *Br. abortus* strain 2308 showed that this agent caused organ burden (total CFU per tissue) in the lungs, with spleen and liver concentrations lagging equally by about an order of magnitude. This reflects the approximate order of magnitude difference between the N_{50} concentrations between the pooled mice-rhesus macaque *Br. melitensis* data and the mice-tested *Br. abortus* bootstrapped dose-response models (Figs. 15 and 16, respectively). Recent comparative analyses done between the complete genomes of *Br. melitensis* (16M), *Br. suis* (1330), and *Br. abortus* (2308) show that although extensive similarity exists between them (>90%), examination of each species' unique genes (often related to phage-mediated integration regions) show 33 regions of >100 base pair fragments are unique. The drive to adapt to host specificity has been proposed to explain these unique gene sequences. Many of these singular conserved sequences relate to virulence factors related to host-specific inactivation of transcriptional regulators and outer membrane proteins.[10,48–50] Mapped phylogenetic trees of these unique gene sequences show that more of them are common to *Br. melitensis* and *Br. abortus* than between *Br. abortus* and *Br. suis.* An attempt to combine the pooled mice-rhesus monkey *Br. melitensis* data (Fig. 14) with the mice *Br. abortus* data (Fig. 16) for a common dose-response model was close to passing the criteria for successful pooling. In contrast, there was a wide divergence in the dose-response data between *Br. suis* and *Br. melitensis* so that creating a pooled dose-response model was not possible. Within the *Brucella* genus, genetic relationships between species and biovars seem to determine observed dose responses. Testing by Elberg and Henderson[25] and Druett *et al.*[22] on *Br. suis* dose responses (Fig. 11) for guinea pigs were done so long ago that it is unclear which one(s) of the five biovars they belonged to. Genetic relationships of the biovars show that four of the biovars (1–4) are closely clustered, except for biovar 5, which is not only phylogenetically distinct from the other *Br. suis* biovars, but is exceptional when compared to all other *Brucella* species. Initial multilocus gene sequence data postulate that this may derive from its being closer to a common *Brucella* ancestor and less evolved than the other groups.[10] Whether taxonomic divisions at a subspecies level based on biovar differences can be phylogenetically meaningful is still to be determined, but it is important to expect differences in their pathogenesis, which may alter their dose-response relationships.

4. CONCLUSION

Dose-response models were created for aerosolized *Br. suis* exposure to guinea pigs from pooled studies (Fig. 11). A parallel pooled dose-response model for guinea pigs inoculated through both aerosol and subcutaneous routes with *Br. melitensis* (Fig. 12) showed that the median infectious dose corresponded to a 30 CFU dose of *Br. suis*, much less than the N_{50} dose of about 94 CFU for *Br. melitensis* organisms.

When the same pathogen (*Br. melitensis*) was tested subcutaneously on mice, the N_{50} correlated dose was higher, 1,840 CFU (Table VI). Crossing species and even administration routes does not seem to impede pooling the dose responses of mice, rhesus macaques, and humans (Table VI; Fig. 15) when exposed to *Br. melitensis* via subcutaneous injection for the animals, and similarly intradermally for humans. Even though *Brucella* species have genetically evolved through their adaptation to different hosts,[10] it seems that it could be likely that invasion of different hosts through the same pathogenic processes is not only possible, but likely. Similar physiological processes are most likely between rhesus macaques and humans since they derived from a recent common ancestor, but the cross-correlation to mice is more unexpected and inexplicable. However, mice are susceptible to all three of the major *Brucella* species that affect humans as well, including *Br. abortus* (bovine) and *Br. suis* (porcine).

It is difficult to extrapolate dose-response models between different species of the same bacterial genus, let alone between different species of test subjects. The challenge of risk assessment is making

reasonable and defensible assumptions in the absence of surety. Although the imminent threat of *Brucella* as a bioterrorism agent demands that general preparedness is mandated,[21] including the construction and utilization of predictive dose-response models, there are many sources of uncertainty remaining. Factors such as aerosol particle size, repeated dosing, and variable virulence between different strains and biovars that are not included in these models can produce large effects on dose and response and should be examined in future clinical trials and modeling efforts.

ACKNOWLEDGMENTS

This research was funded through the Center for Advancing Microbial Risk Assessment, supported by the U.S. Environmental Protection Agency and U.S. Department of Homeland Security, under the Science to Achieve Results grant program (Grant R83236201).

REFERENCES

1. Corbel MJ. Brucellosis: An overview. Emerging Infectious Diseases, 1997; 3:2123–2221.
2. Franco MP, Mulder M, Gilman RH, Smits HL. Human brucellosis. Lancet Infectious Diseases, 2007; 7:775–786.
3. Mantur BG, Mallangouda SB, Bidri RC, Mulimani MS, Veerappa K, Kariholu P, Patil SB, Mangalgi SS. Protean clinical manifestations and diagnostic challenges of human brucellosis in adults: 16 years' experience in an endemic area. Journal of Medical Microbiology, 2006; 55:897–903.
4. Mantur BG, Amarnath SK. Brucellosis in India—A review. Journal of Bioscience, 2008; 33(4):539–547.
5. Young E. Human brucellosis. Review of Infectious Diseases, 1983; 5:821–842.
6. Young E. An overview of human brucellosis. Clinical Infectious Diseases, 1995; 21:283–289.
7. Corbel MJ. Brucella. Pp. 339–353 in Parker MT, Collier LH (eds). Topley and Wilson's Principles of Bacteriology, Virology and Immunology, 8th edition. London, UK: Edward Arnold, 1990.
8. Jahans KL, Foster G, Broughton ES. The characterisation of *Brucella* strains isolated from marine mammals. Veterinary Microbiology, 1997; 57:373–382.
9. Mantur BG, Amarnath SK. Brucellosis in India—A review. Journal of Bioscience, 2008; 33(4): 539–547.
10. Whatmore AM. Current understanding of the genetic diversity of *Brucella*, an expanding genus of zoonotic pathogens. Infection, Genetics and Evolution, 2009; 9:1168–1184.
11. Baldwin CL, Goenka R. Host immune responses to the intracellular bacteria *Brucella*: Does the bacteria instruct the host to facilitate chronic infection? Critical Reviews in Immunology, 2006; 26:407–422.
12. Pappas G, Papdimitriou P, Akritidis N, Christou L, Tsianos EV. The new global map of human brucellosis. Lancet Infectious Diseases, 2006; 6:91–99.
13. Lundervold M, Milner-Gulland EJ, O'Callahan CJ, Hamblin C, Corteyn A, Macmillan AP. A serological survey of ruminant livestock in Kazakhstan during post-Soviet transitions in farming and disease control. Acta Veterinaria Scandinavica, 2004; 45:211–244.
14. Manaseki S. Mongolia: A health system in transition. British Medical Journal, 1993; 307:1609–1611.
15. Roth F, Zinsstag J, Orkhon D, Chimed-Ochir G, Hutton G, Cosivi O, Carrin G, Otte J. Human health benefits from livestock vaccination for brucellosis: Case study. Bulletin of the World Health Organization, 2003; 81:867–876.
16. Trout D, Gomez TM, Bernard BP, Mueller CA, Smith CG, Hunter L, Kiefer M. Outbreak of brucellosis at a United States pork packing plant. Journal of Occupational and Environmental Medicine, 1995; 37(6):697–703.
17. Chomel BB, DeBess EE, Mangiamele DM, Reilly KF, Farver TB, Sun RK, Barrett LR. Changing trends in the epidemiology of human brucellosis in California from 1973 to 1992: A shift toward foodborne transmission. Journal of Infectious Diseases, 1994; 170(5):1216–1223.
18. Ramos JM, Bernal E, Esguevillas T, Lopez-Garcia P, Gaztamibide MS, Gutierrez F. Non-imported brucellosis outbreak from unpasteurized raw milk in Moroccan immigrants in Spain. Epidemiology and Infection, 2008; 136:1552–1555.
19. Munoz PM, Boadella M, Arnal M, de Miguel MJ, Revilla M, Martinez D, Vicente J, Acevedo P, Oleaga A, Ruiz-Fons F, Marin CM, Prieto JM, de la Fuente J, Barral M, Barberan M, Fernandez de Luco D, Blasco JM, Gortazar C. Spatial distribution and risk factors of brucellosis in Iberian wild ungulates. BMC Infectious Diseases, 2010; 10(1):46–60.
20. Centers for Disease Control and Prevention (CDC). Bioterrorism Disease/Agents List. Available at: http://www.bt.cdc.gov/agent/agentlist-category.asp, Accessed on February 4, 2011.
21. Yagupsky P, Baron EJ. Laboratory exposures to brucellae and implications for bioterrorism. Emerging Infectious Diseases, 2005; 11(8):1180–1185.
22. Druett HA, Henderson DW, Peacock S. Studies on respiratory infection. III. Experiments with *Brucella suis*. Journal of Hygiene, 1956; 54(1):49–57.
23. Kleinman LI, Radford Jr, EP. Ventilation standards for small mammals. Journal of Applied Physiology, 1964; 19:360–362.
24. Henderson DW. An apparatus for the study of airborne infection. Journal of Hygiene, 1952; 50(1):53–68.
25. Elberg SS, Henderson DW. Respiratory pathogenicity of *Brucella*. Journal of Infectious Diseases, 1948; 82(3):302–306.
26. Druett HA, Henderson DW, Packman L, Peacock S. Studies on respiratory infection. I. The influence of particle size on respiratory infection with anthrax spores. Journal of Hygiene, 1953; 51(3):359–371.
27. Herzberg M, Elberg SS, Meyer KF. Immunization against *Brucella* infection II. Effectiveness of a streptomycin-dependent strain of *Brucella melitensis*. Journal of Bacteriology, 1953; 66(5):600–605.
28. Herzberg M, Elberg SS. Immunization against *Brucella* infection I. Isolation and characterization of a streptomycin-dependent mutant. Journal of Bacteriology, 1953; 66(5):585–599.
29. Elberg SS, Henderson DW, Herzberg M, Peacock S. Immunization against *Brucella* infection IV. Response of monkeys to injection of a streptomycin-dependent strain of *Brucella melitensis*. Journal of Bacteriology, 1955; 69(6):643–648.
30. Foster JW, Ribi E. Immunological role of *Brucella abortus* cell walls. Journal of Bacteriology, 1962; 84(2):258–268.
31. Pappagianis D, Elberg SS, Crouch D. Immunization against *Brucella* infections. Effects of graded doses of viable attenuated *Brucella melitensis* in humans. American Journal of Epidemiology, 1966; 84(1):21–31.
32. Haas CN, Rose JB, Gerba CP. Quantitative Microbial Risk Assessment. New York: John Wiley, 1999.

33. Abramowitz M, Stegun IA. Pocketbook of mathematical functions. Verlag Harri Deutsch: Thun Frankfurt/Main, 1984.
34. Teunis PFM, Havellar AH. The beta Poisson dose-response model is not a single hit model. Risk Analysis, 2000; 20(4):513–520.
35. Bartrand TA, Weir MA, Haas CN. Dose-response models for inhalation of Bacillus anthracis spores: Interspecies comparisons. Risk Analysis, 2008; 28(4):1115–1124.
36. Huang Y, Bartrand TA, Haas CN, Weir MH. Incorporating time post inoculation into a dose-response model of Yersinia pestis in mice. Journal of Applied Microbiology, 2009; 107:727–735.
37. Huang Y, Haas CN. Time-dose-response models for microbial risk assessment. Risk Analysis, 2009; 29(5):648–661.
38. Tamrakar SB, Haas CN. Dose-response model for *Burkholderia pseudomallei* (meliodosis). Journal of Applied Microbiology, 2008; 105:1361–1371.
39. DeVore JL (ed). Probability and Statistics for Engineering and the Sciences, 6th edition. Belmont, CA: Brooks/Cole-Thomson Learning, 2004, pp. 168–170.
40. Foster G, Osterman BS, Godfroid J, Jacques I, Coeckaert A. *Brucella ceti* sp. nov. and *Brucella pinnipedialis* sp. nov. for *Brucella* strains with cetaceans and seals as their preferred hosts. International Journal of Systematic and Evolutionary Microbiology, 2007; 57:2688–2693.
41. Roy CJ, Hale M, Hartings JM, Pitt L. Impact of inhalation exposure modality and particle size on the respiratory deposition of ricin in BALB/c mice. Inhalation Toxicology, 2003; 15:619–638.
42. Snipes MB. Kinetics of inhaled radionuclides. In Raabe OG (ed). Internal Radiation Dosimetry, Health Physics Society Summer School 1994. Madison, WI: Medical Physics Publishing, 1994.
43. Fiori PL, Mastrandrea S, Rappelli P, Cappuccinelli P. *Brucella abortus* infection acquired in microbiology laboratories. Journal of Clinical Microbiology, 2000; 38(5): 2005–2006.
44. Mense MG, Borshcel RH, Wilhelmsen CL, Pitt ML, Hoover DL. Pathologic changes associated with brucellosis experimentally induced by aerosol exposure in rhesus macaques (*Macaca mulatta*). American Journal of Veterinary Research, 2004; 65(5):644–652.
45. Mantur BG, Mulimani MS, Bidari LH, Akki AS, Takare NV. Bacteremia is as unpredictable as clinical manifestations in human brucellosis. International Journal of Infectious Diseases, 2008; 12:303–307.
46. Izadjoo MJ, Mense MG, Bhattacharjee AK, Hadfield TL, Crawford RM. A study on the use of male animal models for developing a live vaccine for Brucellosis. Transboundary and Emerging Diseases, 2008; 55:145–151.
47. Olsen SC, Waters WR, Stoffregen WS. An aerosolized *Brucella* spp. challenge model for laboratory animals. Zoonoses Public Health, 2007; 54:281–285.
48. Chain PS, Comerci DJ, Tolmasky ME, Larimer FW, Malfatti SA, Vergez LM, Aguero F, Land ML, Ugalde RA, Garcia E. Whole-genome analyses of speciation events in pathogenic Brucellae. Infection and Immunity, 2005; 73: 8353–8361.
49. DelVecchio VG, Kapatral V, Redkar RJ, Patra G, Mujer C, Los T, Ivanova N, Anderson I, Bhattacharyya A, Lykdis A, Reznik G, Jablonski L, Larsen N, D'Souza M, Bernal A, Mazur M, Goltsman E, Selkov E, Elzer PH, Hagius S, O-Callaghan D, Letesson JJ, Haselkorn R, Krypides N, Overbeek R. The genome sequence of the facultative intracellular pathogen *Brucella melitensis*. Proceedings of the National Academy of Sciences USA, 2002; 99:443–448.
50. Halling SM, Peterson-Burch BD, Bricker BJ, Zuerner RL, Qing Z, Li LL, Kapur FV, Alt DP, Olsen SC. Completion of the genome sequence of *Brucella abortus* and comparison to the highly similar genomes of *Brucella melitensis* and *Brucella suis*. Journal of Bacteriology, 2005; 187:2715–2726.